

Towards large-scale restricted active space calculations inspired by the Schmidt decomposition

Gergely Barcza,^{1,2,3} Miklós Antal Werner,^{4,5} Gergely Zaránd,^{5,6} Örs Legeza,^{1,7,8,*} and Tibor Szilvási³

¹*Strongly Correlated Systems Lendület Research Group,*

Wigner Research Centre for Physics, H-1525, Budapest, Hungary

²*Department of Physics of Complex Systems, ELTE Eötvös Loránd University, H-1117, Budapest, Hungary*

³*Department of Chemical and Biological Engineering,*

The University of Alabama, Tuscaloosa, AL-35487, USA

⁴*Budapest University of Technology and Economics,*

Department of Theoretical Physics, Budafoki út 8., H-1111 Budapest, Hungary

⁵*MTA-BME Quantum Dynamics and Correlations Research Group, Institute of Physics,*

Budapest University of Technology and Economics, Budafoki út 8., H-1111 Budapest, Hungary

⁶*BME-MTA Exotic Quantum Phases 'Lendület' Research Group, Institute of Physics,*

Budapest University of Technology and Economics, Budafoki út 8., H-1111 Budapest, Hungary

⁷*Fachbereich Physik, Philipps-Universität Marburg, 35032 Marburg, Germany*

⁸*Institute for Advanced Study, Technical University of Munich,*

Lichtenbergstrasse 2a, 85748 Garching, Germany

(Dated: January 18, 2022)

We present an alternative, memory-efficient, Schmidt decomposition-based extension of the inherently bipartite restricted active space scheme, which can be implemented effortlessly within the density matrix renormalization group method via the dynamically extended active space procedure. Demonstrative calculations are benchmarked against state-of-the-art results of C_2 , which is notorious for its multi-reference character. Besides the uncontracted solution, internal contraction can also be naturally realized in the formalism by keeping only the most relevant Schmidt states.

Introduction. The accurate theoretical description of static electronic structures is provided by the solution of the time-independent Schrödinger equation. In the Born–Oppenheimer approximation, the second quantized representation of the corresponding ab initio Hamiltonian¹ reads

$$\hat{H} = \sum_{ij,\sigma} t_{ij} \hat{a}_{i\sigma}^\dagger \hat{a}_{j\sigma} + \frac{1}{2} \sum_{ijkl,\sigma\sigma'} V_{ijkl} \hat{a}_{i\sigma}^\dagger \hat{a}_{j\sigma'}^\dagger \hat{a}_{k\sigma'} \hat{a}_{l\sigma} + E_{\text{nuc}} \quad (1)$$

with system specific one- and two-electron integrals, t_{ij} , and V_{ijkl} , respectively. Here, operators $\hat{a}_{i\sigma}^\dagger$ and $\hat{a}_{i\sigma}$ create and annihilate one electron with σ spin projection in molecular orbital $i \in \{1, \dots, L\}$. The dimension of the associated computational basis, Φ , increases exponentially with spin-orbital size L , i.e., 4^L , neglecting particle and spin conservation. Therefore, the exact solution on current classical computers is restricted up to around 20 orbitals.²

One protocol that aims to keep the problem of n_e electrons computationally feasible is the complete active space (CAS) scheme^{3–5} which restricts the large configuration space to an effective subset spanned by given $L_{\text{CAS}} \leq L$ orbitals. As illustrated in Fig. 1, the protocol classifies the set of canonical molecular orbitals into three categories: core, active, and virtual. The core and virtual orbitals are kept on the Hartree-Fock level and filled with $n(\Phi_{\text{core}}) = n_{\text{core}}$ and zero electrons, respectively. Note that in this context core orbitals refer to inactive occupied orbitals in general. The active orbitals are populated with the rest of electrons, i.e., $n_a = n_e - n_{\text{core}}$, minimizing the energy. The corresponding determinen-

tal space formally reads

$$\Phi_{\text{CAS}} \equiv \hat{P}_{\text{CAS}} \Phi = \{\Phi_{\text{core}} \Phi_A \in \Phi \mid n(\Phi_A) = n_a\} \quad (2)$$

where the independent conservation of spin channels is not explicitly noted for the sake of brevity. Here, Φ_{core} denotes the string of occupied modes corresponding to the core orbitals while $\Phi_A \in \Phi_A$ iterates on the set of mode configurations given within the subspace of active orbitals, and the operator \hat{P}_{CAS} projects onto the CAS subspace.

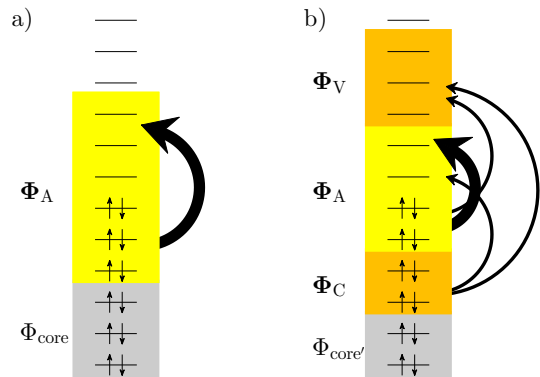


FIG. 1. Schematic illustration of the CAS and RAS concepts. (a) In the CAS scheme the occupation of modes can only change for the active orbitals (A) while occupation of the core and virtual orbitals is frozen. (b) In the RAS scheme, in addition to active orbitals some virtual (V) and core (C) orbitals can also be excited with restrictions: the maximal number of particle excitations in these orbitals is r .

In practical simulations of large systems, a subspace of $L_{\text{CAS}} \ll L$ orbitals is selected to focus on the description of states with strong (static) correlations, i.e., excited configurations that have largest contribution to the ground state. Even though the principal features of the electronic states are characterized by the static correlations, dynamical effects, i.e., contributions of intractable number of highly excited configurations with small weights, can also be crucial to provide an accurate theoretical description that agrees with experimental data.^{6,7} Although CAS level solutions can be combined with lower level methods, e.g., self-consistent field theory, or coupled cluster method, which aim to provide a balanced description of correlation effects^{8,9} these attempts often have unfavorable drawbacks and limitations. In the externally corrected tailored coupled cluster (TCC) method, for example, the full orbital space is split into two parts, CAS and external (EXT). An accurate solution of the CAS is used to obtain a single reference-like wave function for a truncated CC approach to recover a large fraction of the missing dynamical correlations^{10,11}. In spite of the great success of the various embedding methods, their uncontrollable errors often hinder the black box application of them^{12,13}, therefore, development of alternative methods to include the contribution the EXT orbital space is still a major chal-

lenge in computational chemistry.

The restricted active space (RAS) approach, which is practically analogue to the uncontracted multireference configuration interaction, is an alternative to the above mentioned techniques.^{5,14} Conceptually, RAS enhances CAS description by distinguishing two additional subsets of orbitals, i.e., the excitable core (Φ_{C}) and virtual (Φ_{V}) spaces, with the aim of expanding the size of the active space for a manageable computational cost and make active space methods available for larger chemical systems.¹⁵ In these two subsets of orbitals we allow a total of r particle excitations at most. While this restriction drastically reduces the computational dimension demanded by these orbitals, the method can still describe the (weak) dynamical correlations and account for their energy contribution. In the reference (Slater) configuration the activated core orbitals Φ_{C} are completely filled with n_{c} electrons, and the active orbitals are occupied by $n_{\text{e}} - n_{\text{core}'} - n_{\text{c}}$ particles, where $n_{\text{core}'}$ is the number of electrons in the deep core orbitals, $\Phi_{\text{core}'}$, that are still kept at the Hartree-Fock level.

The formally considered $\Phi_{\text{C}} \in \Phi_{\text{C}}$, $\Phi_{\text{V}} \in \Phi_{\text{V}}$ strings of modes are defined within the domain of the core and the virtual subspaces and constrained by maximal r electronic excitations. The associated determinantal space of the RAS scheme is defined as

$$\Phi_{\text{RAS}[r]} \equiv \hat{P}_{\text{RAS}[r]} \Phi = \{\Phi_{\text{core}'} \Phi_{\text{A}} \Phi_{\text{C}} \Phi_{\text{V}} \in \Phi \mid n(\Phi_{\text{A}} \Phi_{\text{C}} \Phi_{\text{V}}) = n_{\text{e}} - n_{\text{core}'} \wedge n_{\text{c}} - n(\Phi_{\text{C}}) + n(\Phi_{\text{V}}) \leq r\}, \quad (3)$$

with $n_{\text{c}} - n(\Phi_{\text{C}})$ the number of holes on the activated core orbitals. The eigenvalue problem of the corresponding Hamiltonian projected from Eq. (1) by $\hat{P}_{\text{RAS}[r]}$ is written as

$$\hat{H}_{\text{RAS}[r]} \Psi_{\alpha} = \hat{P}_{\text{RAS}[r]} \hat{H} \hat{P}_{\text{RAS}[r]} \Psi_{\alpha} = E_{\alpha} \Psi_{\alpha}, \quad (4)$$

where $\Psi_{\alpha} \in \Phi_{\text{RAS}[r]}$ is the α -th many-body eigenstate of the projected Hamiltonian.

Considering a problem characterized by L_{A} , L_{C} , L_{V} number of active, restricted core and virtual spin-orbitals, respectively, at RAS[r] level of theory, the dimension of the associated Hilbert space scales as $\mathcal{O}(4^{L_{\text{A}}}(L_{\text{C}} + L_{\text{V}})^r)$. Hence, diagonalizing large systems is challenged by the footprint of storing the entire Hamiltonian matrix in memory. In order to overcome this limitation, one viable strategy, proposed by the direct-CI approach,^{16,17} is to keep only slices of the matrix in memory during iterative diagonalization.¹⁸

Schmidt decomposed RAS. As an alternative approach to the problem, hereby we propose a novel implementation of the RAS concept which takes advantage of the underlying direct product structure of the retained RAS configuration space. Namely, according to Eq. (3), the computational basis schematically consists of products of configuration states of set Φ_{A} and set $\Phi_{\text{CV}}^{(r)} \equiv \{\Phi_{\text{C}} \Phi_{\text{V}} \in$

$\Phi_{\text{C}} \Phi_{\text{V}} \mid n_{\text{c}} - n(\Phi_{\text{C}}) + n(\Phi_{\text{V}}) \leq r\}$. It is worth to rewrite also the eigenvalue problem of Eq. (4) to emphasize the product structure, i.e.,

$$\begin{aligned} \hat{H}_{\text{RAS}[r]} &= \sum_i \hat{O}_{\text{A}}^{(i)} \otimes \hat{O}_{\text{CV}}^{(i)} \\ \Psi_{\alpha} &= \sum_{\Phi_{\text{A}} \in \Phi_{\text{A}} \Phi_{\text{CV}} \in \Phi_{\text{CV}}^{(r)}} C_{\Phi_{\text{A}} \Phi_{\text{CV}}}^{(\alpha)} \Phi_{\text{A}} \Phi_{\text{CV}} \end{aligned} \quad (5)$$

using Schmidt coefficient matrix $C^{(\alpha)}$ and adequately constructed operators $\hat{O}_{\text{A}}^{(i)}$, $\hat{O}_{\text{CV}}^{(i)}$ acting on subspaces Φ_{A} and $\Phi_{\text{CV}}^{(r)}$, respectively. One major consequence of the Schmidt representation¹⁹ defined in Eqs. 5 is that the consecutive states of the iterative diagonalization via Davidson or Lánczos algorithm, i.e., $\Psi' = \hat{H}_{\text{RAS}[r]} \Psi$, are obtained from the accumulated sum of product of matrices as

$$C^{(\alpha)'} = \sum_i O_{\text{A}}^{(i)} C^{(\alpha)} O_{\text{CV}}^{(i)T}. \quad (6)$$

Here, the dimension of the matrixes reads as $|O_{\text{A}}| = [\mathcal{O}(4^{L_{\text{A}}}), \mathcal{O}(4^{L_{\text{A}}})]$, $|C_{\alpha}| = [\mathcal{O}(4^{L_{\text{A}}}), \mathcal{O}((L_{\text{C}} + L_{\text{V}})^r)]$, $|O_{\text{CV}}| = [\mathcal{O}((L_{\text{C}} + L_{\text{V}})^r), \mathcal{O}((L_{\text{C}} + L_{\text{V}})^r)]$. Consequently for such a bi-partite split, the memory require-

ment of each operator combination might be comparable to the footprint of the sliced-direct-CI method in the regime where $\mathcal{O}(4^{L_A}) \sim \mathcal{O}((L_C + L_V)^r)$. Note that the number of operator combinations is a quadratic function of L_A and $(L_C + L_V)$ for quantum chemical Hamiltonians. For more technical details of the representation see Refs. 20 and 21.

Implementation details. The Schmidt decomposed RAS representation can easily be adapted in the quantum chemical density matrix renormalization group (DMRG) approach^{21–26} through the dynamically extended active space (DEAS) procedure^{27,28} without additional programming efforts. In our implementation, the RAS concept was utilized within the Budapest-DMRG program package²⁹ using the so called two-site variant of DMRG, i.e., the superblock is composed of the updated system block, two orbitals treated exactly and the environment block. In our representation, the system block extended with the two intermediate orbitals spans the configuration space of the active orbitals, Φ_A , and the environment block describes the restricted excitations on core and virtual orbitals, i.e., the corresponding subspace of $\Phi_{CV}^{(r)}$. The sweeping direction in the DMRG method can be reversed for any superblock configuration, thus we perform the sweeping only for the active orbital space and we leave the subspace of $\Phi_{EXT} \equiv \Phi_{CV}^{(r)}$ uncontracted. Since the size of the active block is always much smaller than the size of the environment block, partial summations to form the DMRG auxiliary operators are carried out for the environment block²⁵. The number of basis states used to represent $\Phi_{CV}^{(r)}$ is much larger than the dimension of a single orbital, thus the EXT orbital space can also be considered as a super-site with large dimension attached to the right end of the DMRG chain.

Internal contraction based on von Neumann entropy. In course of the DMRG sweeping procedure, i.e., in the micro iteration steps, the subspace of the system block is truncated by keeping the number of retained basis states, i.e., bond dimension, under control.³⁰ In this work we used both fixed bond dimensions and dynamically adapted values via the dynamical block state selection approach (DBSS) by setting an a priori error margin for the quantum information loss χ .^{27,31} In addition, we also keep representatives of all quantum number sectors in the course of contraction, even those having exactly zero Schmidt values, since these could become particularly relevant in further micro steps and exclusion of them would yield an unresolvable error in the DMRG-RAS procedure.

Benchmark. In the following, as proof of principle, benchmark calculations are presented for the strongly correlated C_2 molecule. Ground state energies obtained with standard quantum chemical methods are compared to the energy calculated by the RAS theory restricted up to two electron excitations ($r = 2$) denoted as RAS-SD-DMRG. The dicarbon is modeled at 1.25 Å bond length in frozen core cc-pVTZ basis³² with $n_e = 12$ and $n_{core} = 4$, i.e. $n_e - n_{core} = 8$ electrons are distributed in 58 orbitals. In our tests, Φ_C is an empty

set, and therefore $\Phi_{CV} = \Phi_V$. The Hartree-Fock electronic structure and the conventional many-body results, i.e., configuration interaction (CI) and coupled cluster expansion (CC) as well as n -valence electron perturbation theory (NEVPT2), are generated using quantum chemical program suite ORCA.³³ The corresponding Hamiltonian matrix elements required for Budapest-DMRG-calculations are provided by MRCC.^{34,35}

In order to study the convergence of the RAS scheme, the number of completely active orbitals is increased in each DMRG micro iteration step from $L_A = 3$ orbitals to 8 of the lowest-lying valence orbitals as seen in Fig. 2. The rest of the valence space is treated on restricted level of theory permitting only at most two electron excitations from the reference HF configuration. Note that the $L_A = 4$ case corresponds to the CI-SD approximation having 4 occupied valence orbitals. The uncontracted RAS-SD-DMRG energy for $L_A = 4 - 8$ active spaces are denoted in blue and the corresponding dimension of the effective configuration space is collected in Fig. 2. We find that the energy drops significantly for $L_A = 5$ where the lowest lying unoccupied molecular orbital of bonding character is added to Φ_A configurational space which also indicates its strongly correlated character. The higher lying virtual orbitals incorporated in $L_A = 6, 7, 8$ active spaces, which all have positive orbital energy and antibonding character, affect less drastically the RAS-SD-DMRG level of solution according to the many-body energy and the wave-function analysis.

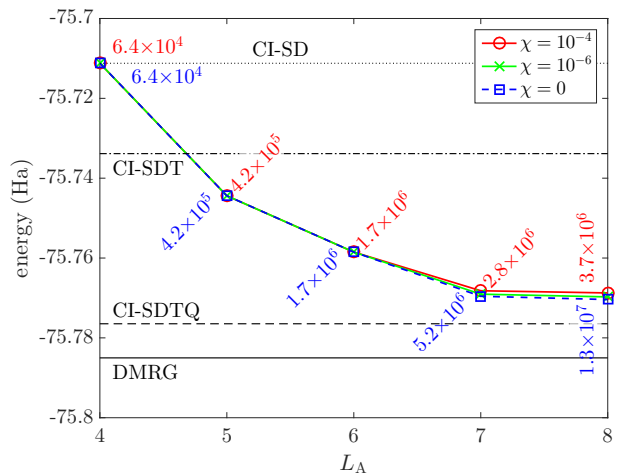


FIG. 2. Ground state energy of dicarbon obtained by RAS-SD-DMRG for increasing L_A subspace in frozen-core cc-pVTZ basis. Dimension of the corresponding RAS configurational space is also shown besides the data points in the figure. The colored lines are guide to the eye. For comparison, reference CI-SD, CI-SDT, CI-SDTQ and large-scale DMRG energy levels are visualized by straight dotted, dashed-dotted, dashed and solid black lines, respectively. For more details of the benchmark test see Tab. I

Applying the modified DBSS truncation scheme, uncontracted RAS-space results, i.e., $\chi = 0$, are readily reproduced within the range of the chemical accuracy for a

fraction of computational cost for truncation thresholds $\chi = 10^{-4}$ and 10^{-6} as depicted in Fig. 2. In particular, for $L_A = 8$ the $M_{\text{exact}} = 4096$ states of the system block is represented by $M = 1300$ many-body states for $\chi = 10^{-4}$ cut-off and the total Hilbert space of the problem is also reduced by a factor of four.

As a comparison, benchmark results of standard post-HF methods are compiled in Tab. I and illustrated in Fig. 2. In particular, modeling the problem at CI-SD, SDT and SDTQ level of theory, the retrieved correlation energy with respect to the DMRG reference correlation energy (obtained using $M = 4096$ and 58 orbitals) increases as 80.8%, 86.7%, 97.8%, respectively. Comparing to the single-reference CI-SD and CI-SDT solutions, RAS-SD-DMRG yields higher resolution of correlations by construction thus lower ground state energy already for $L_A = 5$ setup. On the other hand, setting against the reference CAS-DMRG energy which considers all possible excitations without any restrictions, the RAS-SD-DMRG solution is off by 0.022 Ha for $L_A = 8$ which result translates to 96.2% recovery of the total correlation energy. Notable that CI-SDTQ provides practically exact solution retrieving 97.9% of the correlations.

In Tab. I CC results of various complexity are presented as well. The data clearly demonstrates that the RAS-SD approach computed at modest active space size might not only outperform standard single-reference CI expansions but also cheap CC solutions, i.e., RAS-SD provides more accurate description than CC-SD already for $L_A = 6$. Furthermore, NEVPT2 results are also outperformed using RAS-SD level of theory. Even though the variational RAS based description is computationally more demanding compared to perturbation theory, it might provide more-reliable estimate for strongly correlated problems.

By carrying out further DMRG sweeps restricted to the CAS orbitals only, we have confirmed that the energy can be further minimized. As a proof-of-principle by allowing to merge the subspace of the active orbitals and $\Phi_{\text{CV}}^{(r)}$ through the DMRG backward sweep, $L_A = 8 \rightarrow 3$, but fixing $\min(M) = 5051$ corresponding to $L_{\text{CV}} = 50$, the energy $E = -75.7704$ at the left turning point, $L_A = 3$, was much lower than $E = -75.4942$ obtained by $r = 2$ and $M = 6106$ corresponding to $L_{\text{CV}} = 55$, demonstrating the efficiency of the basis state selection of DMRG. Further sweeps do not change this energy. Performing a similar calculation but using $M = 500$ block states, the exact ($\chi = 0$) RAS-SD result has been reproduced within an error of $\Delta E \approx 0.001$, however with a subspace that is two orders of magnitude smaller. The reference CAS-DMRG calculated with $M = 500$ is also given in Tab. I. Utilizing the DBSS procedure with $\chi = 10^{-4}$ we obtained $\Delta E \approx 10^{-4}$, as expected. In order to study the effect of the number of completely active orbitals we have also performed calculations for L_A up to 18. For $L_A = 14$ the CI-SDTQ energy is recovered with an accuracy of 0.001 with $M = 500$ and for $\chi = 10^{-4}$ even a lower energy bound was reached. In practice, $\Phi_{\text{CV}}^{(r)}$ can also

method	energy (Ha)	Δ_E (%)
HF	-75.4013	0.0
CAS(8,8)	-75.5489	38.5
CI-SD	-75.7112	80.8
CI-SDT	-75.7339	86.7
CI-SDTQ	-75.7765	97.8
CC-SD ^a	-75.7496	90.8
CC-SD(T) ^a	-75.7832	99.5
CC-SDT ^a	-75.7810	99.0
CC-SDTQ ^a	-75.7845	99.9
NEVPT2(8) ^a	-75.7540	91.9
RAS-SD-DMRG(8, $\chi = 10^{-4}$) ^b	-75.7576	92.9
RAS-SD-DMRG(8, $\chi = 0$) ^b	-75.7704	96.2
RAS-SD-DMRG(8, $M = 5051$)	-75.7704	96.2
RAS-SD-DMRG(8, $M = 500$)	-75.7694	95.9
RAS-SD-DMRG(8, $\chi = 10^{-4}$)	-75.7703	96.2
RAS-SD-DMRG(14, $M = 500$)	-75.7753	97.5
RAS-SD-DMRG(14, $\chi = 10^{-4}$)	-75.7792	98.5
RAS-SD-DMRG(18, $M = 500$)	-75.7768	97.8
RAS-SD-DMRG(18, $\chi = 10^{-4}$)	-75.7795	98.6
CAS-DMRG($M = 500$)	-75.7779	98.1
CAS-DMRG($M = 4096$)	-75.7850	100.0

TABLE I. Benchmark test of various post-HF methods for C_2 ground state energy in cc-pVTZ basis using frozen-core approximation. Δ_E stands for the percentage of correlation energy retrieved by the method. Standard CAS-DMRG with retained 4096 block states provides the reference correlation energy (12 electrons on 58 orbitals). Abbreviations are resolved as CI-S/D/T: configuration interaction solution on single/double/triple excitation level; CC: coupled cluster method, NEVPT2: n -electron valence state perturbation theory. ^a denotes the non-variational solutions. NEVPT2 and RAS results are given for $L_A = 8$ and $L_A = 8, 12, 16$, respectively. ^b Corresponds to energy obtained by the first half DMRG sweep to emphasize the gain by the Schmidt decomposition.

method	energy (Ha)
HF	-75.40561
CI-SD	-75.7264
CI-SDT	-75.7497
CC-SD ^a	-75.7656
CC-SD(T) ^a	-75.8007
NEVPT2(8) ^a	-75.7753
RAS-SD-DMRG(8, $\chi = 10^{-6}$) ^b	-75.7749

TABLE II. Similar benchmark test as in Tab. I but for cc-pVQZ basis corresponding to $L = 108$ orbitals.

be included in the sweeping procedure with constraints and an optimal truncated $\Phi_{\text{CV}}^{(r)}$ can be obtained based on quantum information entropies²⁷. For more complex systems ordering optimization can also be applied to select a more appropriate orbitals to the completely active space.

Numerical results for the significantly larger cc-pVQZ

basis set with frozen cores are summarized in Tab. II. Considering the extensive number of orbitals, i.e., $L = 108$, the analysis is restricted to the computationally less demanding methods which confirms trends found in the smaller basis calculations. Most notably, RAS-SD-DMRG after the first half sweep already outperforms CI-SDT and CC-SD at the computationally affordable and chemically motivated L_A active spaces and it produces results comparable to NEVPT2.

Conclusions. In this letter, we proposed a formulation of the restricted active space scheme considering the Schmidt decomposition which can be efficiently treated by the density matrix renormalization group method through the dynamically extended active space (DEAS) procedure without additional programming efforts. The iterative decomposition also provides a possibility to truncate the Hilbert space of the active orbital space using quantum information measures. Most importantly, optimization of the CAS space is carried out in the presence of the EXT space, unlike in case of other embedding methods. As a proof of concept, we tested the method dubbed RAS-SD-DMRG on the strongly correlated problem of dicarbon which is compared to standard state-of-the-art numerical solutions rivaling with respect to accuracy and computational demand.

The generalization of the presented computational scheme as a multilayered protocol is straightforward, i.e., most RAS orbitals are treated only up to double excitation level while the more intricate ones are at higher level of theory. The method is expected to be particularly well-suited to provide a balanced description of static and dynamical correlations of ab initio systems with orbital space separable according to its correlation pattern. The modified dynamical block state selection criteria might also be useful to speed up standard CAS-DMRG convergence as well.

While completing our work we got aware of a similar approach³⁶ suggesting to attach large sites to the two ends of the DMRG chain.

Acknowledgements. This work was supported by the Ministry of Innovation and Technology and the National Research, Development and Innovation Office of Hungary (NKFIH) within the Quantum Information National Laboratory of Hungary and project No. K134983 and No. FK-135496. MAW has also been supported by the ÚNKP-21-4 New National Excellence Program of the Ministry for Innovation and Technology from the source of the National Research, Development and Innovation Fund. The Bolyai Research Scholarship of HAS is greatly acknowledged by G.B. We acknowledge KIFÜ for awarding us access to computational resource based in Hungary. T.S. would like to thank the University of Alabama and the Office of Information Technology for providing high performance computing resources and support that have contributed to these research results. This work was made possible in part by a grant of high-performance computing resources and technical support from the Alabama Supercomputer Authority. Ö.L. also acknowledges financial support from the Hans Fischer Senior Fellowship programme funded by the Technical University of Munich – Institute for Advanced Study. The development of DMRG libraries has been supported by the Center for Scalable and Predictive methods for Excitation and Correlated phenomena (SPEC), which is funded as part of the Computational Chemical Sciences Program by the U.S. Department of Energy (DOE), Office of Science, Office of Basic Energy Sciences, Division of Chemical Sciences, Geosciences, and Biosciences at Pacific Northwest National Laboratory.

Dedicated to the memory of Géza Tichy and János Pipek.

* legeza.ors@wigner.hu

¹ Szabo, A.; Ostlund, N. S. *Modern Quantum Chemistry: Introduction to Advanced Electronic Structure Theory*, 1st ed.; Dover Publications, Inc.: Mineola, 1996.

² Vogiatzis, K. D.; Ma, D.; Olsen, J.; Gagliardi, L.; de Jong, W. A. Pushing configuration-interaction to the limit: Towards massively parallel MCSCF calculations. *The Journal of Chemical Physics* **2017**, *147*, 184111.

³ Roos, B. O. *Advances in Chemical Physics*; John Wiley & Sons, Ltd, 2007; pp 399–445.

⁴ Cramer, C. *Essentials of Computational Chemistry: Theories and Models*; Wiley, 2005.

⁵ Jensen, F. *Introduction to Computational Chemistry*; John Wiley and Sons, Inc.: Hoboken, NJ, USA, 2006.

⁶ Becke, A. D. Density functionals for static, dynamical, and strong correlation. *The Journal of Chemical Physics* **2013**, *138*, 074109.

⁷ Benavides-Riveros, C. L.; Lathiotakis, N. N.; Marques, M. A. L. Towards a formal definition of static and dynamic electronic correlations. *Phys. Chem. Chem. Phys.* **2017**,

19, 12655–12664.

⁸ Olsen, J. The CASSCF method: A perspective and commentary. *International Journal of Quantum Chemistry* **2011**, *111*, 3267–3272.

⁹ Kinoshita, T.; Hino, O.; Bartlett, R. J. Coupled-cluster method tailored by configuration interaction. *The Journal of Chemical Physics* **2005**, *123*, 074106.

¹⁰ Piecuch, P.; Tobol/a, R.; Paldus, J. Approximate account of connected quadruply excited clusters in single-reference coupled-cluster theory via cluster analysis of the projected unrestricted Hartree-Fock wave function. *Phys. Rev. A* **1996**, *54*, 1210–1241.

¹¹ Veis, L.; Antalík, A.; Brabec, J.; Neese, F.; Legeza, Ö.; Pittner, J. Coupled Cluster Method with Single and Double Excitations Tailored by Matrix Product State Wave Functions. *The Journal of Physical Chemistry Letters* **2016**, *7*, 4072–4078.

¹² Faulstich, F. M.; Laestadius, A.; Legeza, Ö.; Schneider, R.; Kvaal, S. Analysis of the Tailored Coupled-Cluster Method in Quantum Chemistry. *SIAM Journal on Numerical Anal-*

- ysis **2019**, *57*, 2579–2607.
- ¹³ Faulstich, F. M.; Mate, M.; Laestadius, A.; Csirik, M. A.; Veis, L.; Antalik, A.; Brabec, J.; Schneider, R.; Pittner, J.; Kvaal, S.; Legeza, Ö. Numerical and Theoretical Aspects of the DMRG-TCC Method Exemplified by the Nitrogen Dimer. *Journal of Chemical Theory and Computation* **2019**, *15*, 2206–2220.
 - ¹⁴ Lischka, H.; Nachtigalova, D.; Aquino, A. J. A.; Szalay, P. G.; Plasser, F.; Machado, F. B. C.; Barbatti, M. Multireference Approaches for Excited States of Molecules. *Chemical Reviews* **2018**, *118*, 7293–7361.
 - ¹⁵ Malmqvist, P. A.; Pierloot, K.; Shahi, A. R. M.; Cramer, C. J.; Gagliardi, L. The restricted active space followed by second-order perturbation theory method: Theory and application to the study of CuO₂ and Cu₂O₂ systems. *The Journal of Chemical Physics* **2008**, *128*, 204109.
 - ¹⁶ Roos, B. O.; Siegbahn, P. *Methods of Electronic Structure Theory. Modern Theoretical Chemistry, vol 3*; Springer: Boston, 1977.
 - ¹⁷ Olsen, J.; Jorgensen, P.; Simons, J. Passing the one-billion limit in full configuration-interaction (FCI) calculations. *Chemical Physics Letters* **1990**, *169*, 463–472.
 - ¹⁸ Davidson, E. R. The iterative calculation of a few of the lowest eigenvalues and corresponding eigenvectors of large real-symmetric matrices. *Journal of Computational Physics* **1975**, *17*, 87–94.
 - ¹⁹ Horodecki, R.; Horodecki, P.; Horodecki, M.; Horodecki, K. Quantum entanglement. *Rev. Mod. Phys.* **2009**, *81*, 865–942.
 - ²⁰ Xiang, T. Density-matrix renormalization-group method in momentum space. *Phys. Rev. B* **1996**, *53*, R10445–R10448.
 - ²¹ White, S. R.; Martin, R. L. Ab initio quantum chemistry using the density matrix renormalization group. *The Journal of Chemical Physics* **1999**, *110*, 4127–4130.
 - ²² Yanai, T.; Kurashige, Y.; Ghosh, D.; Chan, G. K.-L. Accelerating convergence in iterative solution for large-scale complete active space self-consistent-field calculations. *International Journal of Quantum Chemistry* **2009**, *109*, 2178–2190.
 - ²³ Chan, G. K.-L.; Sharma, S. The Density Matrix Renormalization Group in Quantum Chemistry. *Annual Review of Physical Chemistry* **2011**, *62*, 465–481, PMID: 21219144.
 - ²⁴ Wouters, S.; Poelmans, W.; Ayers, P. W.; Neck, D. V. CheMPS2: A free open-source spin-adapted implementation of the density matrix renormalization group for ab initio quantum chemistry. *Computer Physics Communications* **2014**, *185*, 1501 – 1514.
 - ²⁵ Szalay, Sz.; Pfeffer, M.; Murg, V.; Barcza, G.; Verstraete, F.; Schneider, R.; Legeza, Ö. Tensor product methods and entanglement optimization for ab initio quantum chemistry. *Int. J. Quantum Chem.* **2015**, *115*, 1342–1391.
 - ²⁶ Baiardi, A.; Reiher, M. The density matrix renormalization group in chemistry and molecular physics: Recent developments and new challenges. *The Journal of Chemical Physics* **2020**, *152*, 040903.
 - ²⁷ Legeza, Ö.; Sólyom, J. Optimizing the density-matrix renormalization group method using quantum information entropy. *Phys. Rev. B* **2003**, *68*, 195116.
 - ²⁸ Barcza, G.; Legeza, Ö.; Marti, K. H.; Reiher, M. Quantum-information analysis of electronic states of different molecular structures. *Phys. Rev. A* **2011**, *83*, 012508.
 - ²⁹ Legeza, Ö.; Veis, L.; Mosoni, T. QC-DMRG-Budapest, a program for quantum chemical DMRG calculations.
 - ³⁰ White, S. R. Density matrix formulation for quantum renormalization groups. *Phys. Rev. Lett.* **1992**, *69*, 2863–2866.
 - ³¹ Legeza, Ö.; Sólyom, J. Quantum data compression, quantum information generation, and the density-matrix renormalization-group method. *Phys. Rev. B* **2004**, *70*, 205118.
 - ³² Dunning, T. H. Gaussian basis sets for use in correlated molecular calculations. I. The atoms boron through neon and hydrogen. *The Journal of Chemical Physics* **1989**, *90*, 1007–1023.
 - ³³ Neese, F. The ORCA program system. *WIREs Computational Molecular Science* **2012**, *2*, 73–78.
 - ³⁴ Kallay, M. et al. Mrcc, a quantum chemical program suite. 2020; www.mrcc.hu.
 - ³⁵ Kallay, M. et al. The MRCC program system: Accurate quantum chemistry from water to proteins. *The Journal of Chemical Physics* **2020**, *152*, 074107.
 - ³⁶ Larsson, H. R.; Zhai, H.; Gunst, K.; Chan, G. K.-L. Matrix product states with large sites. **2021**,